Earth Sciences
2024, Vol. 13, No. 2, pp. 76-85
https://doi.org/10.11648/j.earth.20241302.14

Research Article

The Application and Effect of AI Fault Interpretation Technology in the Laoyemiao Area

Zeng Cheng[1], Sun Lizhi[2, *], Bi Yongbin[1], Xu Bo[1], Duan Jian[1], Xu Yingxin[2], Qian Liping[2], Zhang Wanfu[2], Zhang Hao[2], Ying Zijuan[2]

[1]Nanpu Oilfield Operation Area, China National Petroleum Corporation Jidong Oilfield Branch, Tangshan, China
[2]Research Institute, Bureau of Geophysical Prospecting INC., China National Petroleum Corporation (BGP), Baoding, China

Abstract

The complex faults, especially mid-deep faults, in the Laoyemiao area of the Nanpu Sag, the Bohai Bay Basin, are unclearly understood for their characteristics, constraining the structural and geological delineation of the area. The hydrocarbon enrichment in the Laoyemiao area is closely related to the faults, and thus the precise identification of mid-deep faults is of great significance for understanding the structural system and reservoir distribution in the area. In the past twenty years, artificial intelligence (AI) scholars developed new technologies and methods to solve engineering problems. Typically, the AI seismic data interpretation technology plays a critical role in improving the accuracy and efficiency of fault interpretation. In order to define the structural characteristics of the Laoyemiao area, the "2W1H" seismic data were processed by fault-constrained structure-oriented filtering, and then interpreted using the EasyTrack module of GeoEast independently developed by BGP. It is found that the imaging quality and accuracy of mid-deep faults are improved effectively. On this basis, the SN-trending strike-slip fault systems were discovered, and the structural pattern and evolution law of mid-deep faults in the Laoyemiao area were re-understood. The results are of great significance for the structural identification, reservoir evaluation and selection of exploration targets in this area.

Keywords

Laoyemiao, Nanpu Sag, AI, Strike-Slip Fault, Structure-Oriented Filtering, Likelihood Attribute, Xinanzhuang Fault

1. Introduction

The Nanpu Sag, in northern Huanghua Depression of the Bohai Bay Basin, is a dustpan-like sag with a half-graben structure that is faulted in the north and overlapped in the south, and a small oil-generation sag developed in the Mesozoic and Cenozoic, under the control of the severe activity of the Xinanzhuang Fault, Baigezhuang Fault, and Gaoliu Fault during the Cenozoic period [1-3]. The Laoyemiao structural belt in the Nanpu Sag lies in the downthrown side of the

*Corresponding author: dqslz@163.com (Sun Lizhi)

Received: 7 December 2023; **Accepted:** 8 April 2024; **Published:** 29 April 2024

middle section of the Xinanzhuang Fault (Figure 1). It is structurally an inherited rollover anticline dominated by the northern boundary fault, and is an important hydrocarbon accumulation area in the Nanpu Sag. Its structure and deposition are obviously controlled by the adjacent Xinanzhuang Fault. The main part of the Laoyemiao structure is characterized by superposition of multi-stage faults [4, 5]. As less uncompartmentalized blocks are found and the exploration is increasingly difficult in the Nanpu Sag, the monolithic structures dominated by the rollover anticline in the Laoyemiao area become favorable replacement targets for oil and gas exploration. However, the well-developed fault system and complex structural evolution are always bottlenecks for drilling success in this area [6]. According to previous studies on the structural styles and their controls over hydrocarbon accumulation in the Nanpu Sag, the formation and evolution of oil and gas reservoirs in the Nanpu Sag are closely related to the distribution and activity of faults [7]. However, there is still a lack of understanding on the characteristics of mid-deep faults and the stacking styles of multi-stage faults in the area, which restricts the determination of favorable exploration and development targets.

Faults were mainly identified using the techniques such as coherence, curvature, and ant body [8]. However, these techniques are not performed satisfactorily in the parts of the Laoyemiao area where the mid-deep seismic data with low signal-to-noise ratio (SNR) are acquired. Especially, the slices of samples from the strata deeper than 3000 m exhibit too low SNR for the evaluation of deep fault distribution and development. In recent years, artificial intelligence (AI) has been preliminarily applied in seismic data interpretation, showing a promising potential [9, 10].

This paper presents an AI fault interpretation technology to identify the strike-slip faults in mid-deep strata of the Laoyemiao area. Specifically, high-quality seismic data are obtained after fault-constrained structure-oriented filtering, and then interpreted using EasyTrack, an AI interpretation module of GeoEast, to predict the faults through deep learning. By applying this technology, a SN-trending fault system was discovered in deep strata of the Laoyemiao area, and it is believed to be controlled by the differential activity of the Xinanzhuang Fault. On this basis, favorable structural traps were found in the wings of the Laoyemiao structural belt, providing additional exploration targets in the Laoyemiao area.

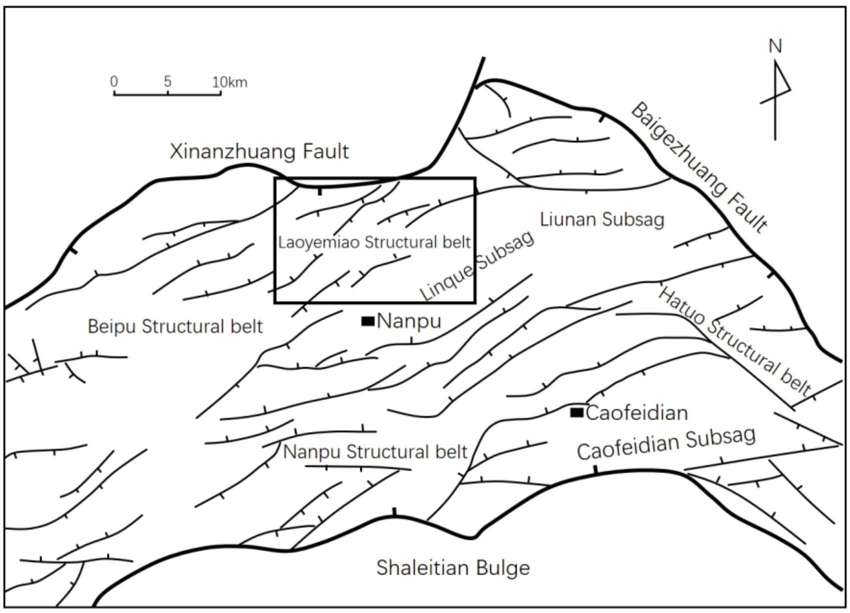

Figure 1. *Location of the Laoyemiao structural belt.*

2. AI Fault Interpretation Technology

AI techniques have been integrated into various disciplines, including seismic data interpretation. Typically, deep learning algorithm is well performed in automatic fault interpretation, horizon auto-tracing, hydrocarbon detection, etc. [11]. Conventional fault interpretation is based on human-computer interaction, with its efficiency and accuracy highly dependent on the experience of interpreters, which increases the cost and risk of oil and gas exploration and development.

The AI fault interpretation technology proposed in this paper includes two steps: (1) fault-constrained structure-oriented filtering, and (2) AI fault prediction based on deep learning, with details shown in Figure 2.

2.1. Fault-Constrained Structure-Oriented Filtering Based on Fault Likelihood Attribute

For the fault-constrained structure-oriented filtering, the post-stack seismic volume is used to estimate the slope (in inline and crossline directions) and flatness attributes of the strata, for subsequent calculation of fault likelihood attribute and structure-oriented smoothing filtering.

The likelihood attribute reflects the possibility of fault existence. It is calculated on the basis of flatness attribute, which is much more accurate than traditional seismic attributes used in fracture prediction based on waveform differences, minimizing the omission of small-scale faults. The fault likelihood attribute *S* is a fault imaging algorithm based on sample processing proposed by Hale in 2013 [12], which is expressed as:

$$s = 1 - \frac{[(d)_s^2]_f}{[(d^2)_s]_f} \tag{1}$$

where, *d* is the 3D seismic volume; *(d)f* denotes another filtering to the seismic volume along the fault trend and strike directions; *(d)s* denotes structure-oriented smoothing to the seismic volume.

When the likelihood attribute values of faults with different azimuths and dip angles at each sampling point are calculated, the maximum likelihood attribute value and corresponding dip angle and azimuth data are retained, so that a multi-information fault likelihood attribute volume is obtained, which is more helpful in calculating the most likely location with fault. Under the constraint of stratigraphic and structural information (including fault and formation), seismic data are adaptively smoothed along the dip and strike of the strata, until a fault structure is encountered. In this way, fault-enhanced seismic data with high signal-to-noise ratio (SNR) are obtained.

2.2. AI Fault Prediction Based on Deep Learning

The EasyTrack module of GeoEast uses deep learning algorithm to realize intelligent fault interpretation. It has been trained with 3D model using big data, forming over a thousand of fault models with various fault properties and corresponding seismic forward modeling data. These fault models include neural network models, such as U-net 3D fault model. The U-net model consists of two sub-nets (encoding sub-net and decoding sub-net), which enable the model to be trained in an end-to-end manner, thereby defining a seismic-based fault prediction model.

The EasyTrack module can predict and generate fault attribute data directly after being loaded with post-stack 3D seismic data, with high computational efficiency. It realizes fault identification from seismic data without excess parameters, which reduces the errors in conventional methods that are dependent on the experience of interpreters. Moreover, the GPU parallel computing technology is coupled to greatly shorten the processing time of fault identification and thus improve the efficiency of seismic data interpretation [13].

This fault prediction method is especially advantageous in fault imaging on vertical seismic section, deep fault imaging, and small fault imaging. It is more effective than the traditional fault imaging techniques based on coherence, variance, and curvature attributes. Therefore, it is expected to become an ideal tool for describing complex faults during fine exploration and efficient development.

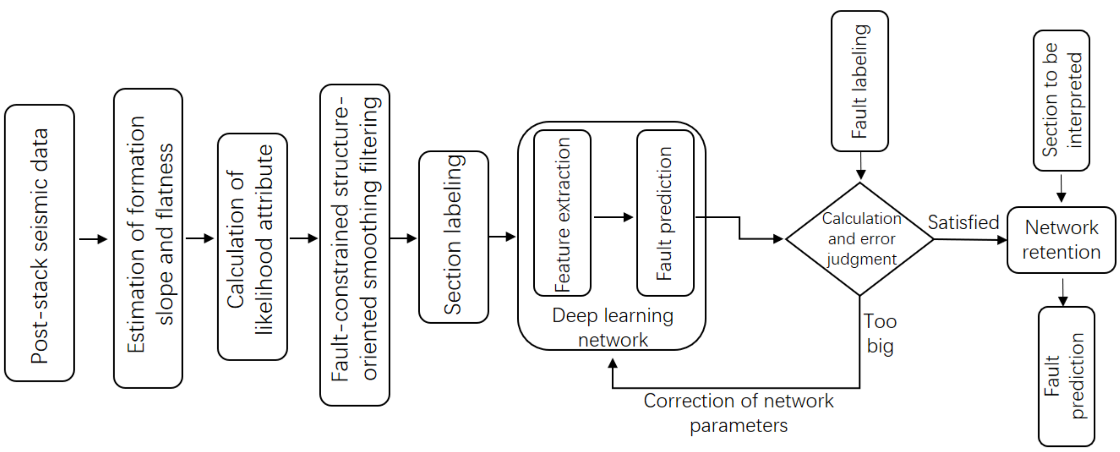

Figure 2. *Process of AI fault interpretation.*

3. Application

This study used the seismic data from the target interval processed in 2021, which are improved in SNR and imaging quality, but fail to evidently reveal the positions of mid-deep fault points/planes. The seismic data were first processed by fault-constrained structure-oriented filtering. The seismic volume reflects significantly smoother seismic events with better continuity, and reveals the faults with apparently enhanced features and better vertical continuity. Furthermore, small faults are imaged effectively, and the fault associations are explicit, making them easily identified and interpreted (Figure 3).

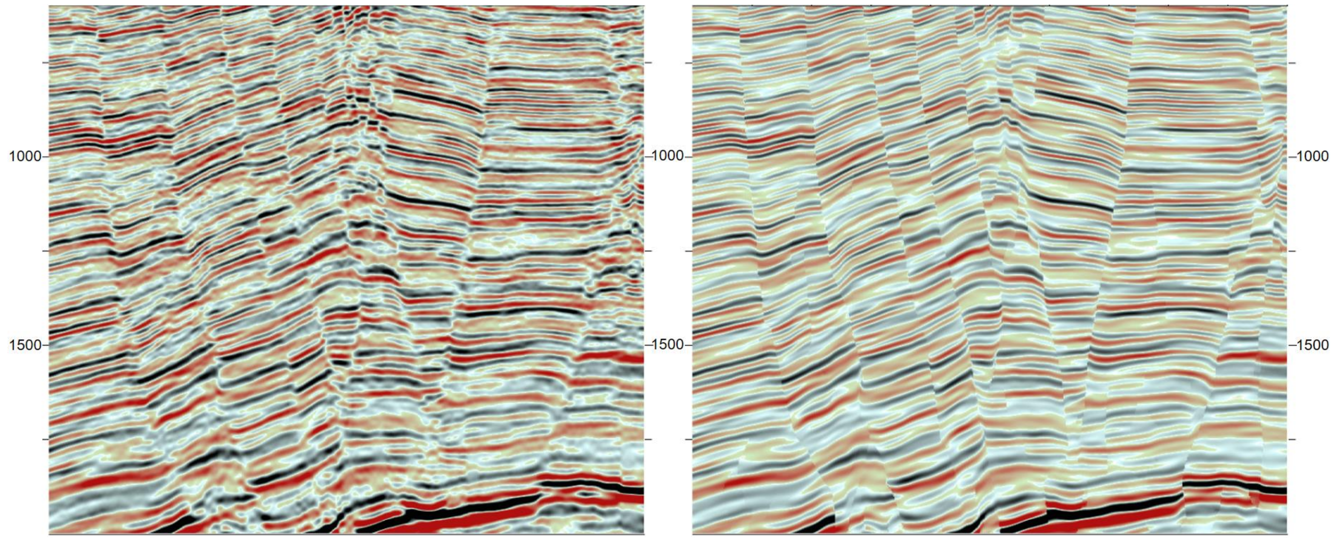

Figure 3. *Seismic section before and after fault-constrained structure-oriented filtering (Left: conventional; Right: filtered).*

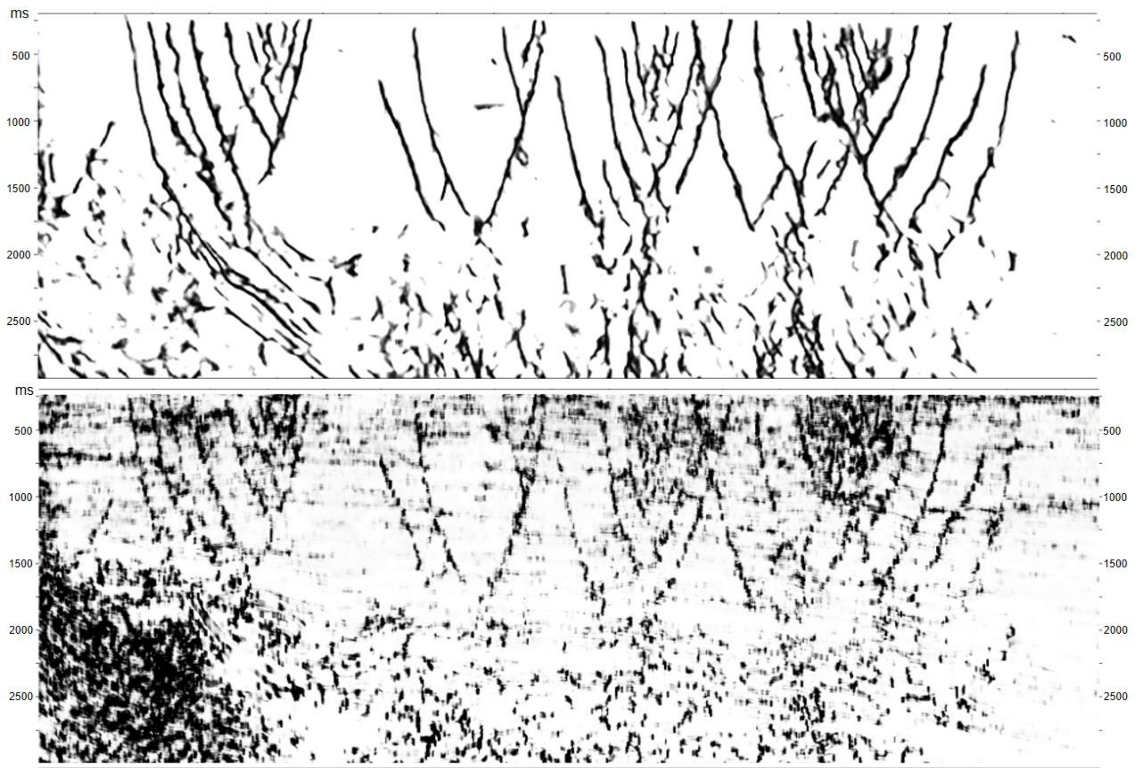

Figure 4. *Seismic sections of the Laoyemiao area (Upper: AI; Lower: coherence).*

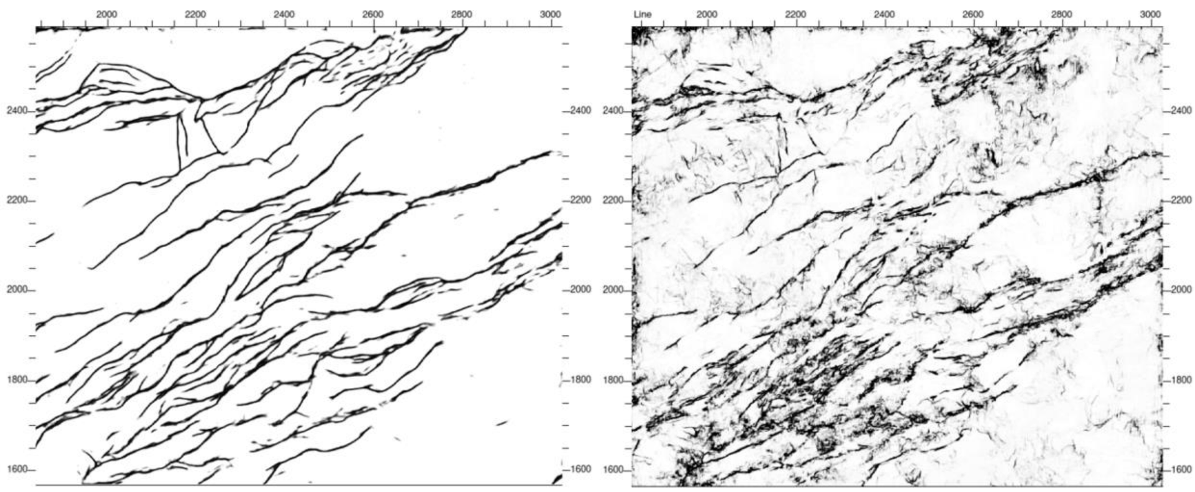

Figure 5. *Slices (1600 ms) of the Laoyemiao area (Left: AI; Right: coherence).*

Then, the training sample model was loaded into the EasyTrack module. The optimal calculation parameters were selected according to the bin size and sampling rate of seismic data, fault responses, and depth of the target layer. The main parameters include sub-volume size, sub-volume overlapping size, resampling ratio, and average velocity. The sub-volume size and sub-volume overlapping size are adjusted depending on the characteristics of the study area and the CPU performance. For example, the sub-volume size can be moderately enlarged for purpose of continuous fault prediction. The average velocity of the target layers is generally 3000–4000 m/s. The resampling ratio can be adjusted to change the calculation efficiency and affect the fault prediction effect, and it will be determined by parameter tests.

The sections obtained by the AI fault interpretation technology above and the coherence attribute analysis were compared (Figure 4). The AI section, with cleaner background, reflects less noise interference, clearer and sharper fault imaging, and more visible fault intersection. In contrast, the coherence attribute section displays fragmented fault planes, with lower continuity and accuracy. Moreover, the AI section shows a more definite five-flower structure, in terms of NW-SE faults cutting through the study area, especially the strike-slip faults with small throws and steeper fault planes. In addition, the AI slice has a higher SNR than the coherence slice, and reveals clearer and more continuous faults in more explicit planar combinations (Figure 5).

4. Results

4.1. Discovery of Mid-Deep SN-Trending Strike-Slip Fault Systems

By using the proposed AI fault interpretation technology, the high-precision fault attribute volume of the Laoyemiao structural belt was established. Figure 6 compares the slices (2660 ms) obtained by AI fault interpretation and conventional coherence analysis. The AI slice reflects clearly two deep fault systems, NE-trending and SN-trending, which intersect obliquely at an angle of nearly 45°. The SN-trending fault system was not detected in previous structural maps. Two sets of nearly SN-trending fault systems can be clearly distinguished in the main part of the Laoyemiao structure: the SN-trending fault system on the west shows high continuity of faults that extend linearly and are overlapped evidently; the SN-trending fault system on the east develops multiple secondary faults parallel or intersecting at small angles with the SN-trending fault system, with each fault extending shortly.

These newly discovered mid-deep SN-trending faults are perpendicular to the Xinanzhuang Fault at the north boundary of the Laoyemiao structural belt, and they are characterized by small dip angle, inherited development, and strong concealment.

Figure 7 shows the slice of the AI fault attribute volume along the plane of the Xinanzhuang Fault. It can be seen that the Xinanzhuang Fault exists obviously in two (east and west) segments, and separated into parts by the SN-trending faults. The presence of numerous SN-trending faults indicates that the Xinanzhuang Fault was highly fractured in the late stage. Totally, 9 nearly SN-trending faults are found, and they distribute in en echelon manner locally (in the early development stage of strike-slip faults). A wide fracture zone can be observed on the section.

Overall, the mid-deep faults (Es–Ed_3) in the Laoyemiao area are supposed to be controlled by oblique transtensional stress, while the Xinanzhuang Fault exhibits dextral strike-slip controlled by transtensional stress. The SN-trending strike-slip faults were almost upright in the early stage, and had relatively small throws in the Dongying period

(Ed). They developed in the Shahejie period (Es), grew continuously in the Dongying period, and was transformed by the NE-trending faults in the Minghuazhen (Nm) and Guantao (Ng) periods (Figure 8).

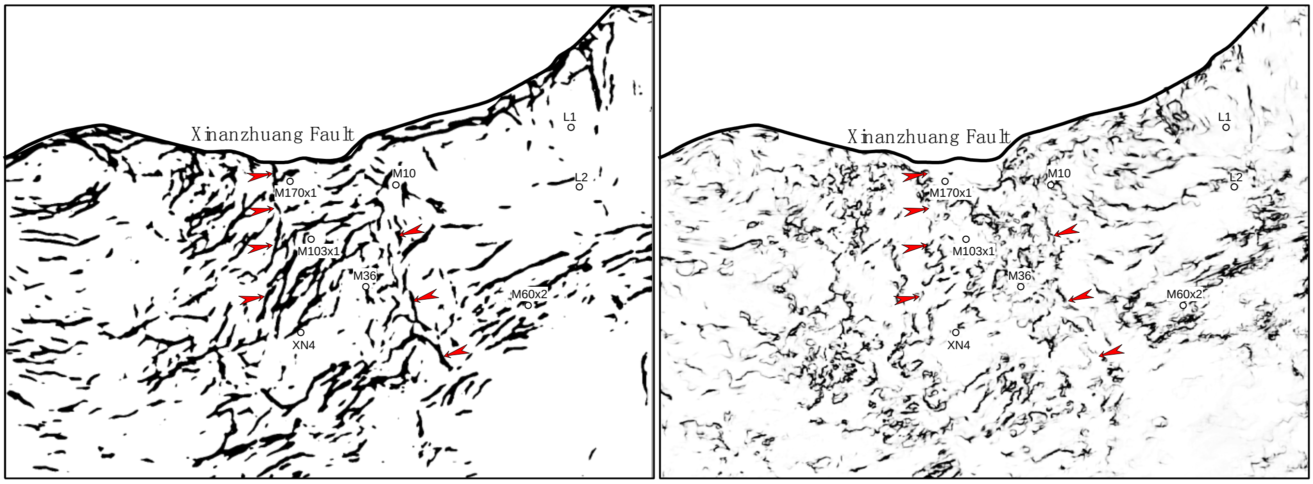

Figure 6. *Slices (2660 ms) of the Laoyemiao area (Left: AI; Right: coherence).*

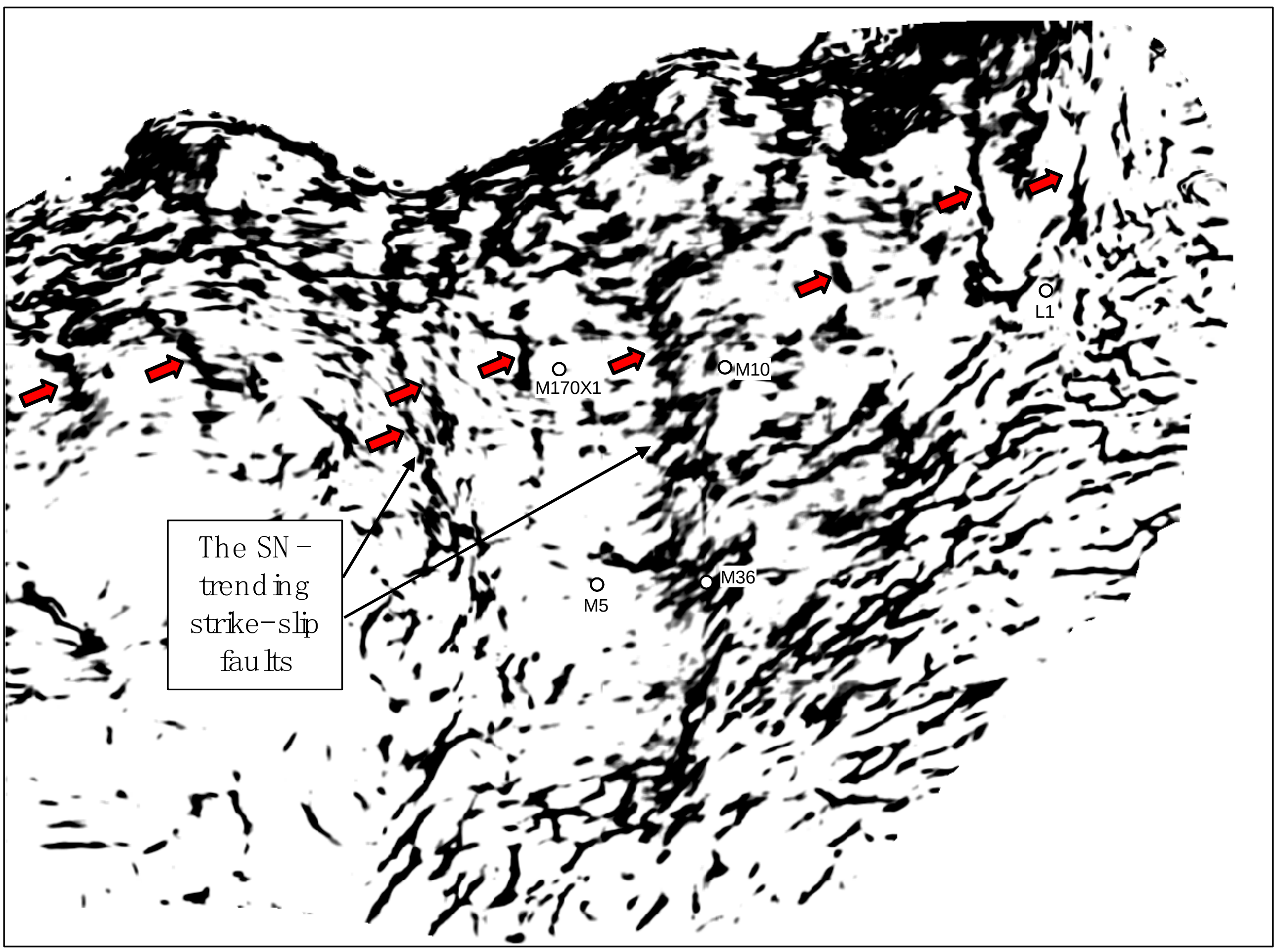

Figure 7. *Slice of AI fault attribute volume of the Laoyemiao area along the plane of Xinanzhuang Fault.*

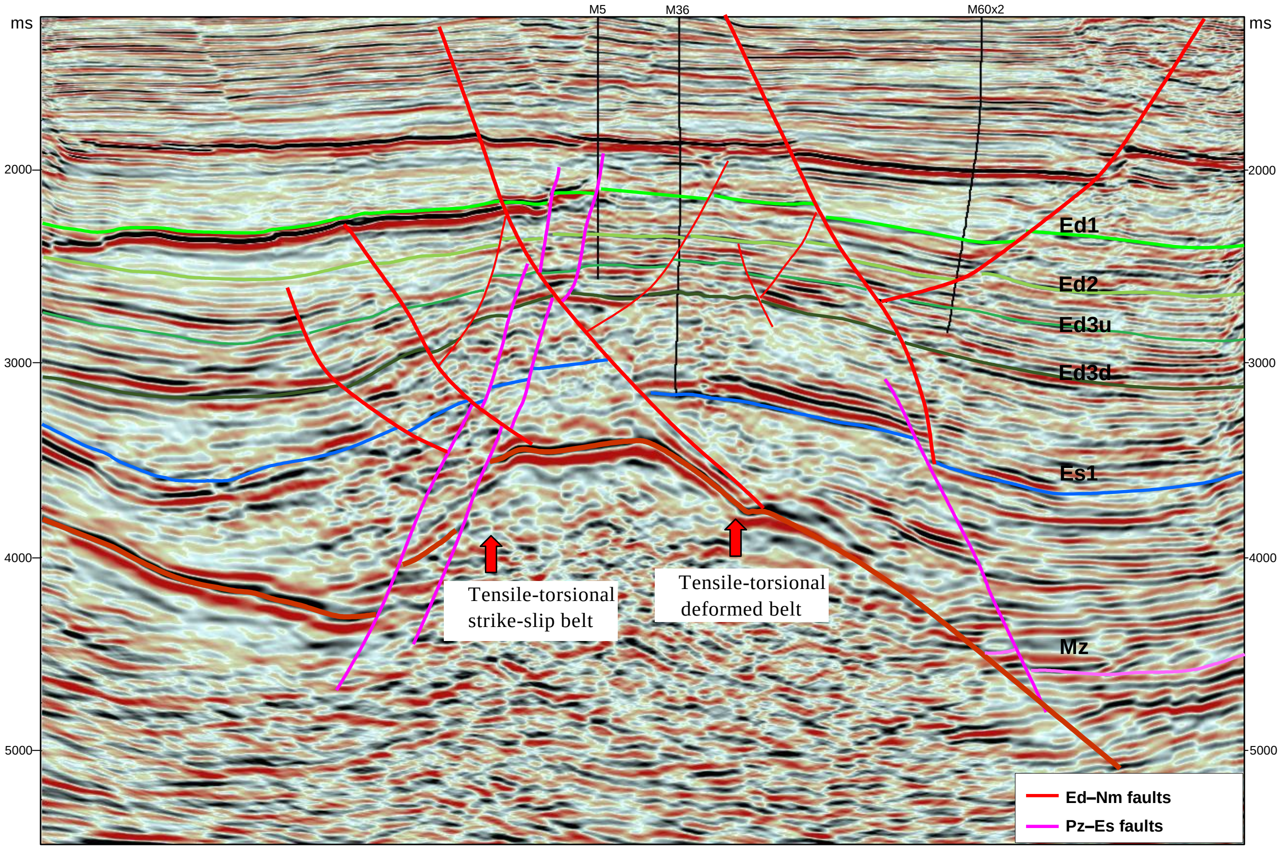

Figure 8. *E-W seismic section through the main part of the Laoyemiao structural belt.*

It is concluded from the above analysis that the deep SN-trending fault systems are controlled by the differential activity of the Xinanzhuang Fault and have the characteristics of dextral strike-slip and late transformation.

4.2. Control of the Differential Activity of the Xinanzhuang Fault on the SN-Trending Fault Systems

The most important fault in the Laoyemiao structure is the northern boundary fault – the Xinanzhuang Fault. Re-analysis using new data suggests that the Xinanzhuang Fault is obviously segmented in the east–west direction. According to the slice of AI fault attribute volume (Figure 9), it is believed that the Xinanzhuang Fault was transformed by a SN-trending strike-slip fault. A deep (4400 ms) slice indicates that the SN-trending fault clearly cuts the Xinanzhuang Fault, which further proves the east–west segmentation of the Xinanzhuang Fault [14].

Along the strike of the Xinanzhuang Fault, it has very different controls on the internal sediments of the sequence. The east segment was developed first, with strong activity in the Sha-1 Member (Es_1) and early Dongying Formation (Ed) periods. The west segment was strongly active during the middle–late Dongying Formation periods, with the dip angle increasing from nearly 60 ° to 80 ° in the east–west direction [15, 16].

From the Es_1 to the early Ed, the stress system became strongly extended in a north-south direction and derived strike-slip components [17]. In the eastern main part of the Laoyemiao structure, during Es_1–early Ed_3, the Xinanzhuang Fault was severely active, with the activity rate much higher than the internal depression rate of the basin. The sedimentary strata at the root of the fault were significantly thickened to form a sub-sag. The formation thickness from the root of the fault to the interior of the sub-sag had a distinct wedge-shaped feature. In the western main part of the Laoyemiao structure, during Es_1–early Ed_3, the Xinanzhuang Fault was weakly active, with the activity rate basically equal to the internal depression rate of the basin. The thicknesses of the Es_1 and Ed_3 at the root of the fault were relatively stable. Due to this differential activity between the western and eastern main parts (Figure 10), nearly S-N shear stress occurred, and dextral strike-slip turned up locally. It is judged that the dextral strike-slip distance of the fault is about 500 m.

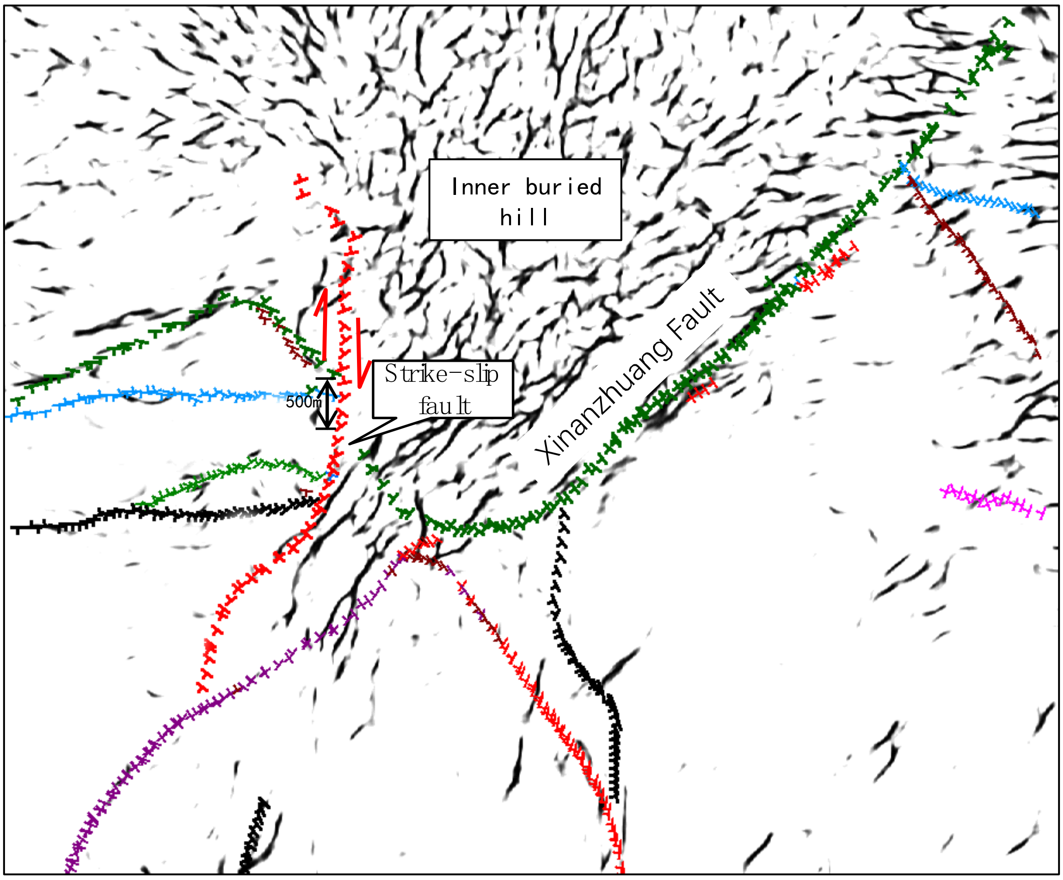

***Figure 9**. Overlap map of AI fault attribute volume slice (4.4 s) and fault points in the Laoyemiao area.*

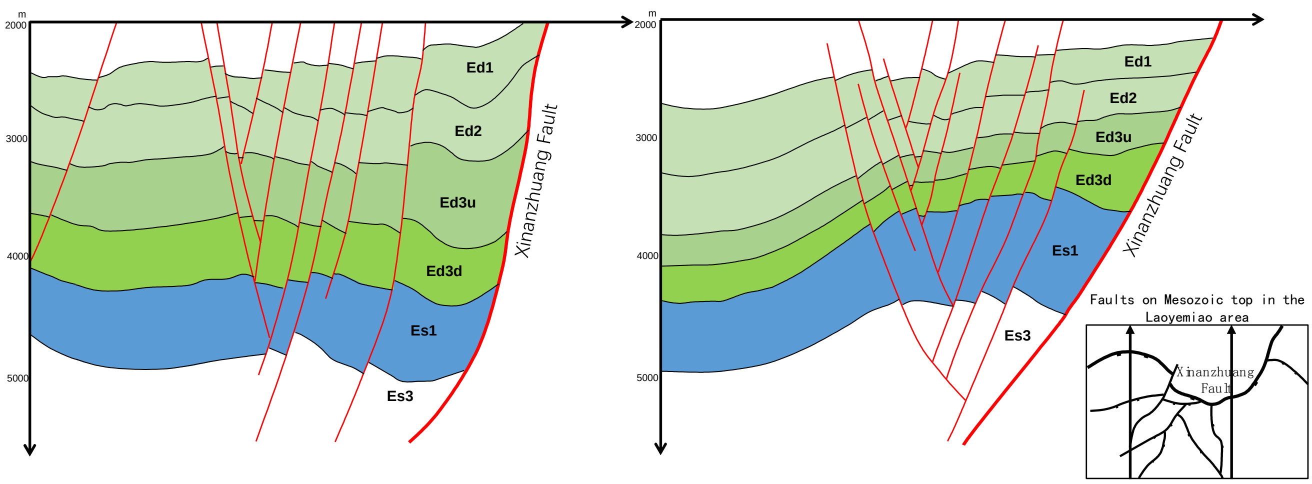

***Figure 10**. Seismic sections of the eastern and western main parts of the Laoyemiao area (Left: western; Right: eastern).*

4.3. Discovery of Favorable Structural Traps in the Wings of the Laoyemiao Structural Belt

Through AI fault interpretation and fine structural interpretation, based on regional geological understanding, the distribution characteristics of Ed_3 faults in the study area were re-investigated, and the control of strike-slip faults on the Ed structure was further clarified. In the Ed, 13 structural traps were newly discovered, with a total area of 4.4 km^2, suggesting a large exploration potential (Figure 11).

A series of faulted-block traps are developed in the western wing of the main part of the Laoyemiao structural belt, with favorable structural conditions, fewer exploration wells, and dominance of lithological and lithological-structural reservoirs. It is recommended to deploy exploration or appraisal wells in favorable areas with well-developed reservoirs, so as to search for new petroliferous blocks.

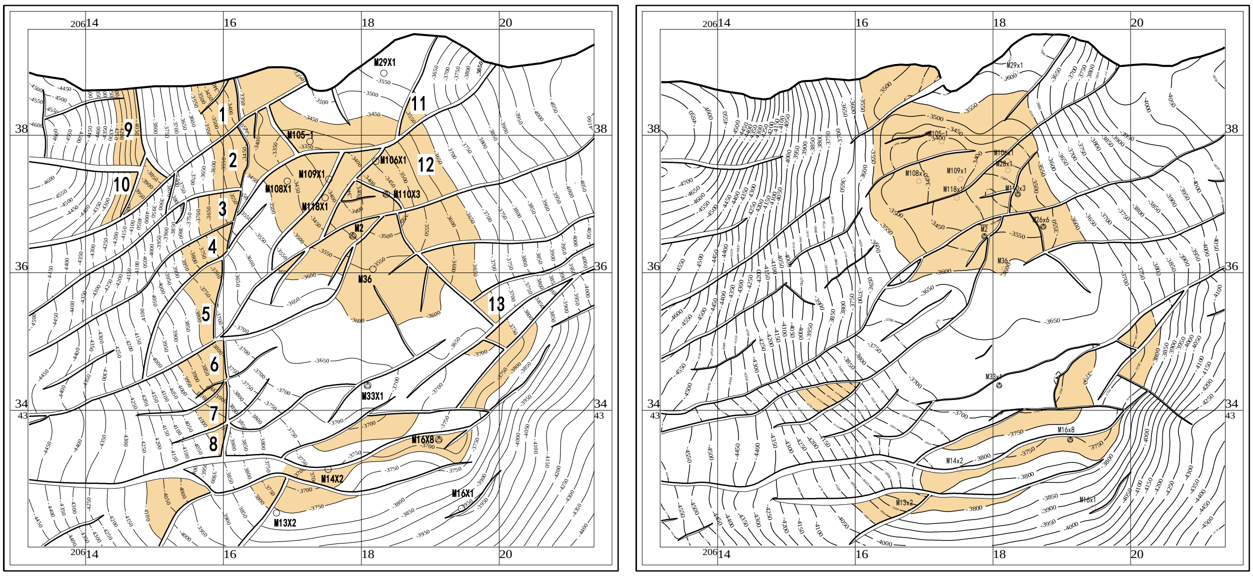

Figure 11. *Bottom structure maps of Ed_3 in the Laoyemiao area (Left: new; Right: old).*

5. Conclusions

Raw seismic data can be processed by structure-oriented filtering based on likelihood attribute to remove high-frequency noise and retain original fault information, thereby highlighting the characteristics of mid-deep faults.

The Laoyemiao structural belt develops complex faults. These intersecting faults, due to severe noise interference in the mid-deep layers, cannot be effectively and efficiently interpreted by conventional interpretation technologies. However, the proposed AI fault interpretation technology accepts model training and does not require excessive manual intervention, making it more advantageous in identifying strike-slip faults with steep occurrence and small throws.

By applying the AI fault interpretation technology, the SN-trending fault systems are newly discovered in the mid-deep strata of the Laoyemiao area, and the mid-deep structural pattern of the Laoyemiao area is re-understood. The study results are of guiding significance for seeking new exploration domains, evaluating reservoirs, and defining exploration targets in the Laoyemiao area.

Conflicts of Interest

The authors declare no conflicts of interest.

References

[1] Liu Lu, Sun Yonghe, Chen Chang, *et al*. Fault reactivation in No. 4 structural zone and its control on hydrocarbon accumulation in Nanpu sag, Bohai Bay Basin, China [J]. Petroleum Exploration and Development, 2022, 49(04): 716-727. https://doi.org/10.11698/PED.20220056

[2] Zhou Haimin, Wei Zhongwen, Cao Zhonghong *et al*. Relationship between formation, evolution and hydrocarbon in Nanpu Sag [J]. Oil&Gas Geology, 2000(04): 345-349. https://doi.org/10.13247/j.cnki.jcumt.001000

[3] Cong Liangzi, Zhou Haimin. Polyphase pulls and aparts of active rift in Nanpu Depression and their relationship with oil and gas [J]. Oil&Gas Geology, 1998(04): 30-35. https://doi.org/10.11743/ogg19980406

[4] Liu Haiqing, Jin Pengbo, Liu Jingdong *et al*. The fault characteristics of the Laoyemiao structural belt in the Nanpu Depression and its control on hydrocarbon accumulation [J/OL]. Geology in China, 2023, 3: 1-13. https://doi.org/10.12029/gc20220910001

[5] Sun Simin, Ji Hancheng, Liu Xiao *et al*. Architecture of sequence stratigraphy responding to segmentation of boundary fault: taking an example of Dongying Formation on hanging wall of Xinanzhuang Fault in Nanpu Sag [J]. Journal of Jilin University (Earth Science Edition), 2017, 47(02): 382-392. https://doi.org/10.13278/j.cnki.jjuese.201702105

[6] Liu Xingke, Gan Huajun, Chen Si. Evolution of sedimentary system of continental faulted lacustrine basin under high-precision sequence framework: A case from the third member of Dongying Formation in Laoyemiao area, Nanpu Sag [J]. Geological Science and Technology Information, 2019, 38(03): 88-102. https://doi.org/10.3799/dqkx.2020.064

[7] Wu Jizhong, He Shumei, Yang Qianqian *et al*. Research on low-order fault interpretation method based on fully convolutional neural network (FCN) [C]. SPG/SEG, Nanjing, 2020: 1010-1012. https://doi.org/10.3390/jmse9030259

[8] Yang Ping, Song Qianggong, Zhan Shifan *et al*. Research and industrial application of efficient structural interpretation technology based on deep learning [J]. Oil Geophysical Prospecting, 2022, 57(06): 1265-1275+1255. https://doi.org/10.11648/j.ijepe.20231204.11

[9] Ren Wei, Shuai Jian. The application of artificial intelligence in fracture mechanics-crack identification, diagnosis and prediction [J]. Mechanics in Engineering, 2023, 45(01): 1-9. https://doi.org/10.6052/1000-0879-22-401

[10] Zhao Bangliu, Yong Xueshan, Gao Jianhu *et al*. Progress and development direction of PetroChina intelligent seismic processing and interpretation technology [J]. China Petroleum Exploration, 2021, 26(05): 12-23. https://doi.org/10.3969/j.issn.1672-7703.2021.05.002

[11] Yang Yong. Application progress of big data & AI technologies in exploration and development of Shengli Oilfield [J]. Petroleum Geology and Recovery Efficiency, 2022, 29(01): 1-10. https://doi.org/10.13673/j.cnki.cn37-1359/te.2022.01.001

[12] Hale Dave. Methods to compute fault images, extract fault planes, and estimate fault throws from 3D seismic images [J]. Geophysics, 2013, 78(2): 33-43. https://doi.org/10.1190/geo2012-0331.1

[13] Chen Weichang, Yan Jingjing, Sun Guanyu *et al*. Fault tectonics and petroleum entrapment in the Laoyemiao Region of the Nanpu Depression [J]. Journal of Southwest Petroleum University (Science & Technology Edition), 2018, 40(02): 46-56. https://doi.org/10.11885/j.issn.1674-5086.2016.11.04.02

[14] Sun Simin, Ji Hancheng, Wang Jianwei *et al*. Segmentation characteristics and evolution of Xinanzhuang fault in Nanpu Sag, Bohai Bay Basin [J]. Petroleum Geology & Experiment, 2016, 38(05): 628-634. https://doi.org/10.11781/sysydz201605628

[15] Jiang Hua, Wang Jianbo, Zhang Lei *et al*. Segment activity of Xi'nanzhuang Fault in Nanpu Sag and its controlling on sedimentary process [J]. ACTA Sedimentologica SINICA, 2010, 28(06): 1047-1053. https://doi.org/10.14027/j.cnki.cjxb.2010.06.004

[16] Dong Yuexia, Wang Zecheng, Zheng Hongju *et al*. The control of strike-slip faulting on the formation of oil and gas reservoirs in the Nanpu Sag [J]. Petroleum Exploration and Development, 2008(04): 424-430. https://doi.org/10.1016/S1876-3804(08)60090-7

[17] Liu Xiaowen, Chang Di, Shi Shangming. Structure analysis of the Paleogene strata in the northern Nanpu sag: The “transfer growth” phenomenon in fault links and its significance [J]. Journal of China University of Mining & Technology, 2018, 47(06): 1287-1294. https://doi.org/10.13247/j.cnki.jcumt.000847